Kinetics of the Iodine Transfer Polymerization of Vinylidene Fluoride

CYRILLE BOYER, DAVID VALADE, PATRICK LACROIX-DESMAZES, BRUNO AMEDURI, BERNARD BOUTEVIN

Laboratoire de Chimie Macromoléculaire, Ecole Nationale Supérieure de Chimie de Montpellier (UMR 5076-CNRS), 8 Rue de l'Ecole Normale, 34296 Montpellier Cedex 1, France

Received 16 May 2006; accepted 23 June 2006
DOI: 10.1002/pola.21654
Published online 29 August 2006 in Wiley InterScience (www.interscience.wiley.com).

ABSTRACT: The kinetics of the iodine transfer polymerization (ITP) of vinylidene fluoride (VDF) was achieved in the presence of three different chain-transfer agents (CTAs): 1-iodoperfluorohexane ($C_6F_{13}I$), 1-iodo-2*H*,2*H*-perfluorooctane ($C_6F_{13}CH_2CF_2I$), and 1,1,2,2-tetrafluoro-3-iodopropane ($HCF_2CF_2CH_2I$). ITPs of VDF carried out in the presence of $C_6F_{13}I$ and $C_6F_{13}CH_2CF_2I$ showed the following: (1) a linear increase in DP_n versus α_{VDF}, which evidenced the controlled character of ITP, although the polydispersity indices were slightly high (ca 1.5), and (2) theoretical DP_n values close to the targeted ones. In contrast, neither of these statements was observed for the ITP of VDF in the presence of $HCF_2CF_2CH_2I$ achieved under the same conditions, even if the synthesized oligomers could be reactivated. Although the C_{Tr} values of $C_6F_{13}I$ and $C_6F_{13}CH_2CF_2I$ were close (i.e., 7.7 at 75 °C), that of $HCF_2CF_2CH_2I$ was lower (0.3 at 75 °C). The percentages of $-CF_2I$ and $-CH_2I$ functionalities were also assessed, and in the course of the reaction, a reduction of $-CF_2I$ end groups was noted. Then, the mechanism of the ITP of VDF was proposed. © 2006 Wiley Periodicals, Inc. J Polym Sci Part A: Polym Chem 44: 5763–5777, 2006

Keywords: degree of polymerization (DP); fluoropolymers; living polymerization; molecular weight distribution/molar mass distribution; NMR; radical polymerization

INTRODUCTION

Though discovered in the late 1970s,[1–3] controlled free-radical polymerization attracted much interest in the mid 1990s.[4] This is based on adding to a polymerization medium a species able to react with active centers by reversible termination[4–7] or transfer.[1–3,8–13] Hence, equilibrium occurs between the living radicals (or active species) and dormant (or nonpropagating) species. A radical polymerization can be called controlled when the three following conditions are fulfilled:[4]

1. The controlling species must be quickly consumed, and this consumption rate must be faster than that of the propagation step.
2. The polymeric chain must be created in a short time and not in the course of the polymerization, as in the traditional process.
3. The dormant (P—X) and active ($P^{\bullet}$) species must exchange quickly (Scheme 1).

In the last decade, nitroxide-mediated polymerization,[5] atom transfer radical polymerization,[6,7] and methods based on transfer [reversible addition–frag-

This article includes Supplementary Material available from the authors upon request or via the Internet at www.interscience.wiley.com/jpages/0887-624X/suppmat.

Correspondence to: B. Ameduri (E-mail: bruno.ameduri@enscm.fr)

Journal of Polymer Science: Part A: Polymer Chemistry, Vol. 44, 5763–5777 (2006)
©2006 Wiley Periodicals, Inc.

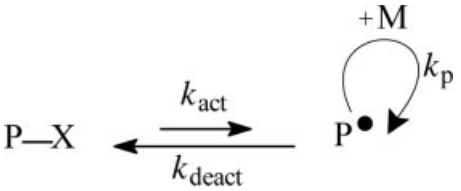

Scheme 1. General scheme for reversible activation in controlled radical polymerization.

mentation chain transfer (RAFT),[12,13] macromolecular design by interchanges of xanthates,[10,11] and iodine transfer polymerization (ITP)[1,2,8,9,14]] have been the three main emerging approaches.

Nowadays, ITP of fluorinated alkenes is a technique that enables various companies involved in fluorine chemistry to produce fluorinated thermoplastic elastomers (TPEs), which have been recently reviewed.[14] These TPEs are diblock or triblock copolymers composed of hard and soft sequences prepared by the stepwise (or sequential) ITP of various fluoroalkenes. They have been marketed by Daikin,[8,15] Dupont,[16,17] and Ausimont[18–20] (now Solvay Solexis) under the Daiel, Viton, and Tecnoflon trademarks, respectively. These triblock copolymers [based on a large variety of different monomeric units such as vinylidene fluoride (VDF), hexafluoropropylene, chlorotrifluoroethylene, tetrafluoroethylene, perfluoromethyl vinyl ether, ethylene, and propylene or a combination of two or three of these alkenes][3,18–21] can be synthesized because of the controlled behavior of that radical polymerization in the presence of a fluoroiodinated transfer agent. Besides, ITPs of other monomers have also confirmed their controlled character in the presence of alkyl iodides. These monomers are mainly hydrogenated, such as styrene,[22] methyl acrylate,[23] butyl acrylate,[23–26] vinyl acetate,[27] vinylidene chloride,[28] and vinyl chloride.[29–45] Although many industrial breakthroughs have been achieved, leading to various patents, ITP of fluorinated alkenes has been described in a few articles[1–3,9] and in a chapter of a book.[14] Nowadays, the evidence of the controlled character of that polymerization (especially the linear relationship between the molar masses of the resulting polymers and the monomer conversions) deserves to be proved, even if the kinetics of these gaseous fluoroalkenes seem more difficult to be determined than those of liquid, hydrogenated monomers.

In a recent article,[46] the microstructure of oligo-VDFs is studied. This article considers the influence of defects of VDF chaining on the control of ITP, especially because the produced reversed —CF_2CH_2I end group can be reactivated with difficulty. This inversion was evidenced by the choice of three chain-transfer agents (CTAs) representing the possible end structures of growing chains: 1-iodoperfluorohexane ($C_6F_{13}I$), 1-iodo-2*H*,2*H*-perfluoro-octane ($C_6F_{13}CH_2CF_2I$), and 1,1,2,2-tetrafluoro-3-iodopropane ($HCF_2CF_2CH_2I$). In contrast to those observed from the last one, the first two lead to a good fit between the targeted and experimentally observed number-average degree of polymerization (DP_n) values. Thus, it was worth investigating the kinetics of the ITP of VDF and assessing the values of the transfer constant (C_{Tr}) of these three CTAs at different temperatures. Then, it was also of interest to determine the ratio of the square of the propagation rate coefficient (k_p) to the termination rate coefficient (k_{te}) of VDF in the radical polymerization. These are the objectives of this article.

EXPERIMENTAL

Materials

VDF (or 1,1-difluoroethylene; bp = −82 °C) and 1,1,1,3,3-pentafluorobutane were kindly offered by Solvay S.A. (Tavaux, France, and Brussels, Belgium). $HCF_2CF_2CH_2I$ (purity = 99%) was purchased from Aldrich Chimie (Saint Quentin-Fallavier, France), and $C_6F_{13}I$ or perfluorohexyliodide (purity = 99%) were generously supplied by Atofina (now Arkema; Pierre-Benite, France). They were worked up with sodium thiosulfate and then distilled before use. *tert*-Butylperoxypivalate (TBPPI; purity = 75%) and 2,5-dimethyl-2,5-bis(*tert*-butylperoxide)hexane (DHBP; purity = 90%) were gifts from Akzo Nobel (Chalons sur Marne, France). They were used as supplied. Acetonitrile, dimethylformamide (DMF), tetrahydrofuran, methanol, methyl ethyl ketone, and dimethylacetamide (DMAc) (analytical-grade) were purchased from Aldrich Chimie.

$C_6F_{13}CH_2CF_2I$ was synthesized by the thermal telomerization of VDF with $C_6F_{13}I$ at 200 °C for 12 h, and this monoadduct was purified by distillation, as previously reported.[47] It was worked up with sodium thiosulfate and then distilled before use.

Analyses

The compositions and structures of the oligomers obtained by ITP were determined with ^{19}F and ^1H NMR spectroscopy. The NMR spectra were

10990518, 2006, 19, Downloaded from https://onlinelibrary.wiley.com/doi/10.1002/pola.21654 by Cochrane Japan, Wiley Online Library on [30/05/2023]. See the Terms and Conditions (https://onlinelibrary.wiley.com/terms-and-conditions) on Wiley Online Library for rules of use; OA articles are governed by the applicable Creative Commons License

recorded on Bruker AC 200, AC 250, and 400 (200-, 250-, and 400-MHz) instruments with deuterated acetone, dimethyl sulfoxide (DMSO), or DMF as the solvent and tetramethylsilane (or $CFCl_3$) as the reference for ^1H (or ^{19}F) nuclei. Coupling constants and chemical shifts are given in hertz and parts per million, respectively. The experimental conditions for ^1H (or ^{19}F) NMR spectra were as follows: a flip angle of 90° (or 30°), an acquisition time of 4.5 s (or 0.7 s), a pulse delay of 2 s (or 5 s), 16 (or 64) scans, and a pulse width of 5 μs (for ^{19}F NMR).

Size exclusion chromatography (SEC) analyses were performed with a Spectra-Physics apparatus equipped with two PLgel 5-μm mixed-C columns from Polymer Laboratories and a Spectra Physics SP8430 refractive-index detector {the signals assigned to PVDF–I [where PVDF is poly(vinylidene fluoride)] gave negative values}. DMAc was chosen as the eluent at 70 °C with a flow rate of 0.6 mL min^{-1}. The standards were monodispersed polystyrene purchased from Polymer Laboratories.

Matrix-assisted laser desorption/ionization time-of-flight (MALDI-TOF) was performed with an Ultraflex Bruker (Université de Montpellier II) in the reflectron mode (accelerating potential of 20 kV) on a Bruker apparatus equipped with a nitrogen laser (337 nm). 2,3,4,5,6-Pentafluorocinnamic acid and sodium iodide (NaI) (or silver trifluoroacetate AgTFA) were used as the matrix and the cationizing agent, respectively. The concentrations of the sample and matrix solutions were 10 g L^{-1} in DMF, and the analyte/matrix ratio was 1/10 (v/v). The mixture (1 μL) was deposited on a stainless steel target, air-dried, and introduced into the spectrometer *in vacuo*.

Reaction in an Autoclave

ITPs of VDF were performed in the presence of $C_6F_{13}I$, $C_6F_{13}CH_2CF_2I$, or $HCF_2CF_2CH_2I$ as the CTA and initiated with TBPPI at 75 °C or DHBP at 135 °C according to a procedure described in the supplementary material.

After purification, the samples were characterized with ^{19}F and ^1H NMR spectroscopy. For example, for ^{19}F NMR [deuterated acetone, δ (ppm)] of $C_6F_{13}CH_2CF_2$–$(VDF)_n$–I (DP_n = 13; experimental conditions for the ITP of VDF with $C_6F_{13}CH_2CF_2I$: $[VDF]_0/[C_6F_{13}CH_2CF_2I]_0/[TBPPI]_0$ = 100.0:6.6:0.6 at 75 °C), we found.

^{19}F NMR: −38.0 (t, —CH_2—CF_2I, 1.2F); −60.0 (m, —CF_2—CF_2I, 0.0F); −82.0 (m, CF_3—CF_2—, 3.0F); −91.0 (m, —CH_2—CF_2— CH_2—CF_2—, 23.1F); −95.7 (m, CH_3—CH_2—CF_2—, 0.0F); −108.0 (m, CH_3—CF_2—, —CF_2—CF_2— CH_2I, —CF_2—CF_2—CH_2—CF_2—, 0.8F); −112.0 [m, $(CH_3)_3$ C—CF_2—CH_2—, 2.7F]; −113.4 (m, —CH_2—CF_2 —CF_2—CH_2—CH_2—, 2F); −114.8 (dm, —CH_2— CF_2H, 0.0F); −115.7 (m, —CH_2 —CF_2—CF_2—CH_2—CH_2—, 0.0F). ^1H NMR: 1.0 [s, $(CH_3)_3CCH_2$—CF_2—, 0.0H]; 1.2 (t, CH_3—CH_2—CF_2—, 0.0H); 1.3 [s, $(CH_3)_3$ C—CF_2—CH_2—, 0.0H]; 1.8 (t, CH_3—CF_2— CH_2—, 0.0H); 2.3 (m, —CH_2—CF_2—CF_2—CH_2—C H_2—CF_2—, 0.4H); 2.9 [m, —CH_2—CF_2—CH_2—CF_2—CH_2—CF_2—, CH_3—CH_2—CF_2—, $(CH_3)_3$CCH_2—CF_2—, 21.5H]; 3.3 (q, $^3J_{HF}$ = 15 Hz, C_6F_{13}—CH_2—CF_2—, 2.0H); 3.7 (q, $^3J_{HF}$ = 14.0 Hz, —CH_2—CF_2I, 1.1H); 3.9 (q, $^3J_{HF}$ = 8.0 Hz, —CF_2—CH_2I, 0.9H); 6.5 (t, $^2J_{HF}$ = 49.6 Hz, $^3J_{HF}$ = 4.0 Hz, HCF_2CF_2—, 0.0H).

For example, we determined ^{19}F and ^1H NMR [deuterated acetone, δ (ppm)] for the oligomer obtained by the ITP of VDF with $HC_2F_4CH_2I$ (DP_n = 35; recorded in deuterated DMF, 400 MHz, 298 K; experimental conditions for the ITP of VDF with $HC_2F_4CH_2I$: $[VDF]_0/[HC_2F_4CH_2I]_0/[TBPPI]_0$ = 100.0:6.6:0.6 at 75 °C).

^{19}F NMR: −38.0 (t, —CH_2—CF_2I, 0.0F); −91.0 (m, —CH_2—CF_2—CH_2—CF_2—, 78.0F); −95.7 (m, CH_3—CH_2—CF_2—, 2.0F); −108.0 (m, CH_3—CF_2—, —CF_2—CF_2—CH_2I, —CF_2—CF_2—CH_2—CF_2—, 1.9F); −112.0 [m, $(CH_3)_3$C—CF_2—CH_2—, 2.7F]; −113.4 (m, —CH_2—CF_2—CF_2—CH_2—CH_2—, 5.5F); −114.8 (dm, —CH_2—CF_2H, 0.0F); −115.7 (m, —CH_2 —CF_2—CF_2—CH_2—CH_2—, 5.5F), −136.0 (d, —CF_2— CF_2H, 2.0F). ^1H NMR: 1.0 [s, $(CH_3)_3CCH_2$—CF_2—, 0.1H]; 1.2 (t, CH_3—CH_2—CF_2—, 0.2H); 1.3 [s, $(CH_3)_3$C—CF_2—CH_2—, 0.2H]; 1.8 (t, CH_3—CF_2 —CH_2—, 0.4H); 2.3 to 2.9 (m, —CH_2—CF_2—CF_2—CH_2—CH_2—CF_2—, m, —CH_2—CF_2—CH_2—CF_2—CH_2—CF_2—, CH_3—CH_2—CF_2—, $(CH_3)_3$CCH_2—CF_2—, 82.0H); 3.3 (q, $^3J_{HF}$ = 15 Hz, C_6F_{13} —CH_2—CF_2—, 0.0H); 3.7 (q, $^3J_{HF}$ = 14.0 Hz, —CH_2 —CF_2I, 0.0H); 3.9 (q, $^3J_{HF}$ = 8.0 Hz, —CF_2—CH_2I, 2.0H); 6.5 (t, $^2J_{HF}$ = 49.6 Hz, $^3J_{HF}$ = 4.0 Hz, HCF_2CF_2—, 1.0H).

Kinetics of the ITP of VDF

Aliquots were periodically sampled from the autoclave (with a probe) in the course of the polymerization of VDF to monitor the following: (1) the conversions of both the monomer and the CTA and (2) the evolution of the molar masses. The collected samples were frozen into liquid nitrogen to stop the

10990518, 2006, 19, Downloaded from https://onlinelibrary.wiley.com/doi/10.1002/pola.21654 by Cochrane Japan, Wiley Online Library on [30/05/2023]. See the Terms and Conditions (https://onlinelibrary.wiley.com/terms-and-conditions) on Wiley Online Library for rules of use; OA articles are governed by the applicable Creative Commons License

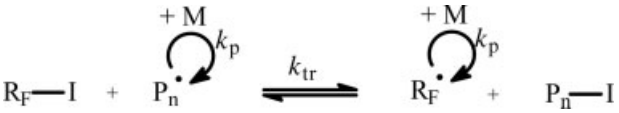

Scheme 2. Chain-transfer reaction in ITP (R_F represents C_6F_{13}, $C_6F_{13}CH_2CF_2$, or $HCF_2CF_2CH_2$).

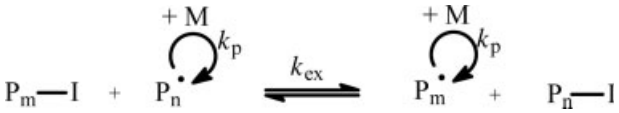

Scheme 3. Exchange reaction in ITP.

polymerization reaction and then diluted in DMAc and were characterized with SEC and NMR.

RESULTS AND DISCUSSION

Concept of ITP

ITP is a degenerative transfer polymerization requiring alkyl iodides:[23] an initiating radical ($A^\bullet$), generated by the thermal decomposition of a conventional radical initiator, reacts with a monomer (M) and leads to a propagating radical ($P_n^\bullet$; direct initiation). This mechanism exhibits two transfer reactions:

1. The first one deals with the exchange of iodine from the transfer agent, R_F—I, to the propagating macroradical, $P_n^\bullet$, resulting in the formation of the polymeric alkyl iodide, P_n—I, and in a new initiating radical, $R_F^\bullet$ (first transfer reaction, Scheme 2). The ratio of the transfer rate coefficient (k_{tr}) to k_p is called C_{Tr}, which gives the intrinsic reactivity of the transfer agent. The reactivity of the CTA is defined by this value. Indeed, a high C_{Tr} value (i.e., >1) means that the CTA allows the molar masses of the resulting polymers to be controlled.
2. The second transfer reaction concerns the exchange reaction between $P_n^\bullet$ and P_m—I (Scheme 3). This reaction allows the growing chains to react with additional monomeric units in each activation–deactivation cycle. Ideally, in ITP, to lead to a polymer with a narrow molar mass distribution, the exchange rate coefficient has to be higher than the propagation rate coefficient [exchange constant (C_{ex}) >1].[23,48] Litvinenko and Muller[49] showed that the value of the polydispersity index (PDI) depends on C_{ex} and can be approximated at a high monomer conversion as follows: $PDI = 1 + [CTA]_0/[M]_0 + (1/C_{ex}) \approx 1 + (1/C_{ex})$.

Thus, in the ITP mechanism, C_{Tr} indicates the activity of the CTA. Therefore, the amount of the CTA controls the number of chains and, hence, the molar masses of the oligomers (in the ideal case, e.g., when the chains formed by direct initiation from the initiator can be neglected).

In this work, the ITP of VDF was carried out in the presence of three fluorinated CTAs initiated with TBPPI at 75 °C (Scheme 4).

In each case, the reaction was monitored via sampling in the autoclave. The targeted DP_n values were low enough (DP_n = 15–30) to allow the formation of soluble oligomers to be easily characterized with SEC in DMAc and with ^{19}F NMR spectroscopy (deuterated DMF was used as the solvent). The former technique enabled us to determine the relative molar masses and their polydispersities, whereas the latter one allowed us to assess the conversions of both the monomer and CTA, DP_n, and the nature of the end groups.

ITP of VDF in the Presence of $C_6F_{13}I$

The VDF conversion (α_{VDF}) was determined by ^{19}F NMR; we took into account the signals centered at −83.0, −91.0, −38.0, and −108.0 ppm, which were assigned to CF_3 in the C_6F_{13} end group, to CF_2 of VDF units in PVDF–I, and to —CH_2CF_2I and —CF_2CH_2I end groups, respectively.[46] As the initial amount of VDF (i.e., the quantity of VDF introduced into the autoclave) was known, α_{VDF} could be assessed:

$$\alpha_{VDF} = \frac{\left(\int CF_2^{-38.0ppm} + \int CF_2^{-91.0ppm} + \int CF_2^{-108.0ppm} + \int CF_2^{-113ppm} + \int CF_2^{-116ppm}\right)/2}{\left(\int CF_3^{-83.0ppm}\right)/3} \times \frac{[CTA]_0}{[VDF]_0} \quad (1)$$

10990518, 2006, 19, Downloaded from https://onlinelibrary.wiley.com/doi/10.1002/pola.21654 by Cochrane Japan, Wiley Online Library on [30/05/2023]. See the Terms and Conditions (https://onlinelibrary.wiley.com/terms-and-conditions) on Wiley Online Library for rules of use; OA articles are governed by the applicable Creative Commons License

$$C_6F_{13}\text{-}I + n CF_2{=}CH_2 \xrightarrow[75\ ^\circ C]{TBPPI} C_6F_{13}{-}CH_2\text{-}CF_2{-}(VDF)_{n\text{-}1}\text{-}I \quad (a)$$

$$C_6F_{13}CH_2CF_2\text{-}I + n\ CF_2{=}CH_2 \xrightarrow[75\ ^\circ C]{TBPPI} C_6F_{13}CH_2CF_2{-}(VDF)_n\text{-}I \quad (b)$$

$$HCF_2CF_2CH_2\text{-}I + nCF_2{=}CH_2 \xrightarrow[75\ ^\circ C]{TBPPI} HCF_2CF_2CH_2{-}(VDF)_n\text{-}I \quad (c)$$

Scheme 4. Synthesis of PVDF–I oligomers by the ITP of VDF in the presence of different CTAs initiated with TBPPI.

where $\int CF_x^{-i\text{ppm}}$, $[CTA]_0$, and $[VDF]_0$ represent the integral of the signal assigned to the CF_x group centered at $-i$ ppm and the concentrations of CTA and VDF at $t = 0$, respectively.

Interestingly, the ^{19}F NMR spectrum shows only traces of both multiplets centered at −113.0 and −116.0 ppm, which were assigned to $—CH_2C\mathit{F}_2—C\mathit{F}_2CH_2—CH_2CF_2—$ reversed head-to-head addition.[46]

The $C_6F_{13}I$ conversion (α_{C6F13I}) could also be calculated from ^{19}F NMR by the monitoring of the decrease in the integral of the signal centered at −60.0 ppm (characteristic of the $—CF_2I$ end group in $C_6F_{13}I$) and that of the signal located at −83.0 ppm, which was attributed to the $CF_3—$ end group:

$$\alpha_{C_6F_{13}I} = \frac{\left(\int CF_3^{-83.0\text{ppm}}\right)\Big/3 - \left(\int CF_2 - I^{-60.0\text{ppm}}\right)\Big/2}{\left(\int CF_3^{-83.0\text{ppm}}\right)\Big/3} \quad (2)$$

After 10 min at 75 °C (α_{VDF} was ca. 25%) in the presence of TBPPI, $C_6F_{13}I$ was totally converted.

Figure 1 presents the evolution of DP_n versus α_{VDF}, showing that the higher α_{VDF} was, the higher DP_n was. The experimental number-average degree of polymerization ($DP_{n,^{19}F\ NMR}$) was assessed with ^{19}F NMR spectroscopy:

$$DP_{n,^{19}F\ NMR} = (\alpha_{VDF} \times [VDF]_0)/(\alpha_{CTA} \times [CTA]_0) \quad (3)$$

where α_{CTA} is the CTA conversion. Interestingly, the experimental DP_n linearly increased with the monomer conversion, and this evidenced the controlled character of that reaction [Fig. 1(a)].[4] This figure clearly demonstrates the controlled character of the ITP of VDF, and this is the first time that this behavior has been reported in the literature. In addition, the experimental values of DP_n were close to the theoretical number-average degree of polymerization ($DP_{n,theoretical}$) values, which were determined as follows:

$$DP_{n,theoretical} = (\alpha_{VDF} \times [VDF]_0)/[CTA]_0 \quad (4)$$

where $[VDF]_0$ and $[CTA]_0$ represent the initial concentrations of VDF and the CTA ($C_6F_{13}I$ in this case), respectively.

The controlled character of the ITP of VDF with $C_6F_{13}I$ was also confirmed with SEC chromatograms of sampled PVDF–I. As expected, the SEC signals assigned to PVDF–I were negative. The SEC chromatograms were shifted to lower elution volumes, that is, to higher molar masses [Fig. 2(a)]. This behavior is typical of a controlled character and also corresponds to a high C_{Tr} value.[49,50]

Because it is usually difficult to get absolute values of the molar masses of fluoropolymers (a lack of standards), the structures of the polymers obtained by the ITP of VDF in the presence of $C_6F_{13}I$ were further studied with MALDI-TOF (Fig. 3). Figure 3 exhibits the spectrum of C_6F_{13}–$(VDF)_n$–I oligomers and shows a series of peaks separated by 64 Da (corresponding to the molecular weight of one VDF unit). This population was centered at 1193 Da (n = 10).

The MALDI-TOF spectrum of the expected C_6F_{13}–$(VDF)_n$–I/Ag^+ structure exhibits signals centered at 1001.88(n = 7), 1065.90(n = 8), 1129.94 (n = 9) and others containing an increment of 64 Da. Interestingly, there is an absence of peaks assigned to oligomers such as $(CH_3)_3C$–$(VDF)_{n+m}$–$C(CH_3)_3/Ag^+$,$(CH_3)_3C$–$(VDF)_n$–I/Ag^+,CH_3–$(VDF)_n$–I/Ag^+,$(CH_3)_3C$–$(VDF)_{n+m}$–CH_3/Ag^+, and CH_3–$(VDF)_{n+m}$–CH_3/Ag^+, which could be obtained by direct initiation from a radical arising from the decom-

10990518, 2006, 19, Downloaded from https://onlinelibrary.wiley.com/doi/10.1002/pola.21654 by Cochrane Japan, Wiley Online Library on [30/05/2023]. See the Terms and Conditions (https://onlinelibrary.wiley.com/terms-and-conditions) on Wiley Online Library for rules of use; OA articles are governed by the applicable Creative Commons License

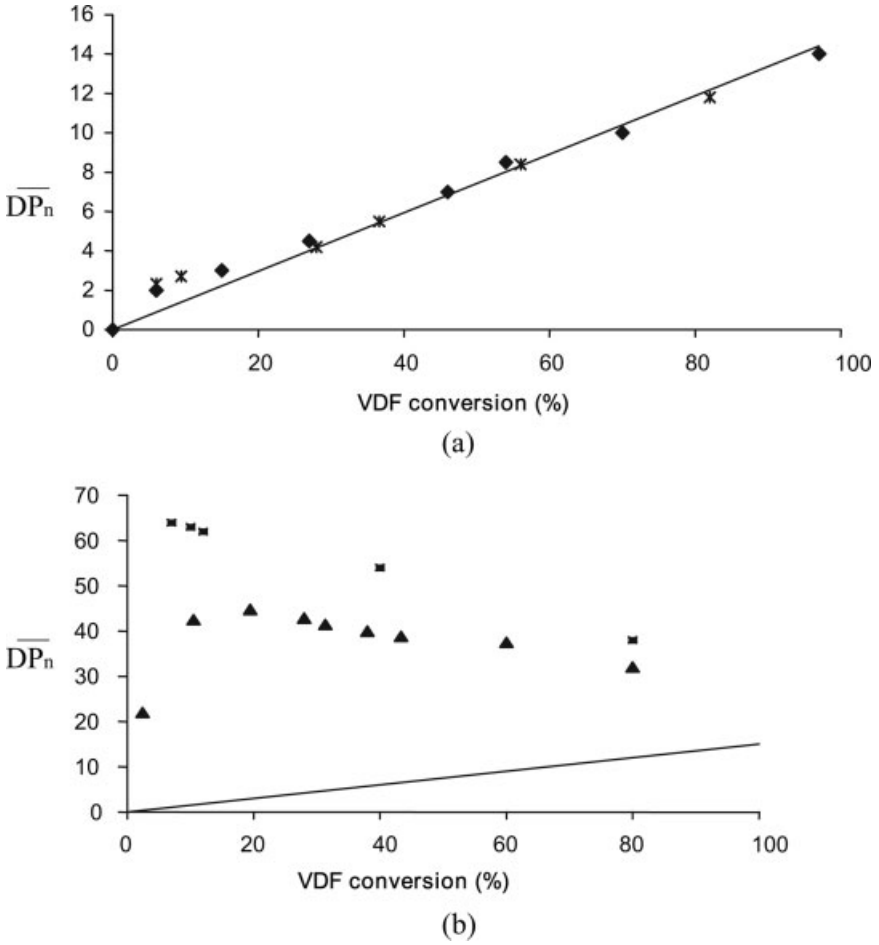

Figure 1. Variations of DP_n versus the monomer conversion for the ITP of VDF performed with different CTAs and at two temperatures (targeted $DP_n = 15$): (a) at 75 °C with (◆) $C_6F_{13}I$ and (×) $C_6F_{13}CH_2CF_2I$ and (b) with $HCF_2CF_2CH_2I$ at (■) 75 and (▲) 135 °C. The straight lines represents the theoretical DP_n values.

position of TBPPI [$CH_3^{\bullet}$ or $^{\bullet}C(CH_3)_3$].[51] These results confirm those found by ^{19}F and ^{1}H NMR characterizations (see Figs. 4 and 5 in the supplementary material).

ITP of VDF in the Presence of $C_6F_{13}CH_2CF_2I$

This CTA was chosen for checking its reactivity in the ITP of VDF because its $—CH_2CF_2I$ end group mimics a PVDF–I model. It also completes this investigation when it is compared with $HCF_2CF_2CH_2I$, which also exhibits an isomeric VDF–I end group (reversed unit). It was worth comparing the reactivity of the iodine atom in both these models because the chemical environments are different.

$C_6F_{13}CH_2CF_2I$ was synthesized by the thermal telomerization of VDF with $C_6F_{13}I$ at 200 °C for 12 h, and this monoadduct was purified by distillation, as previously reported.[47] As expected, the ^{19}F NMR spectrum shows, besides the unchanged chemical shift of the fluorinated groups in the $CF_3(CF_2)_4—$ group, the absence of a signal centered at −60.0 ppm characteristic of $C_5F_{11}CF_2I$ and the presence of that signal centered at −38.0 ppm assigned to the $—CH_2CF_2I$ end group.[47,52]

As previously stated, in the ITP of VDF in the presence of $HCF_2CF_2CH_2I$, α_{CTA} was monitored with ^{19}F NMR on sampled aliquots. Indeed, the chemical shift of $—CH_2CF_2I$ underwent a slight low-field shift from −39.8 to −38.6 ppm [Fig. 4(a)]. Interestingly, the ^{19}F NMR spectrum exhibits the chemical shifts of the $—CH_2CF_2I$ end groups of the monoadduct, diadduct, triadduct, and higher adducts centered at −39.8, −39.1, −38.7 and −38.6 ppm, respectively. Incidentally, the quintet observed for the peak assigned to $—CH_2CF_2I$ in

10990518, 2006, 19, Downloaded from https://onlinelibrary.wiley.com/doi/10.1002/pola.21654 by Cochrane Japan, Wiley Online Library on [30/05/2023]. See the Terms and Conditions (https://onlinelibrary.wiley.com/terms-and-conditions) on Wiley Online Library for rules of use; OA articles are governed by the applicable Creative Commons License

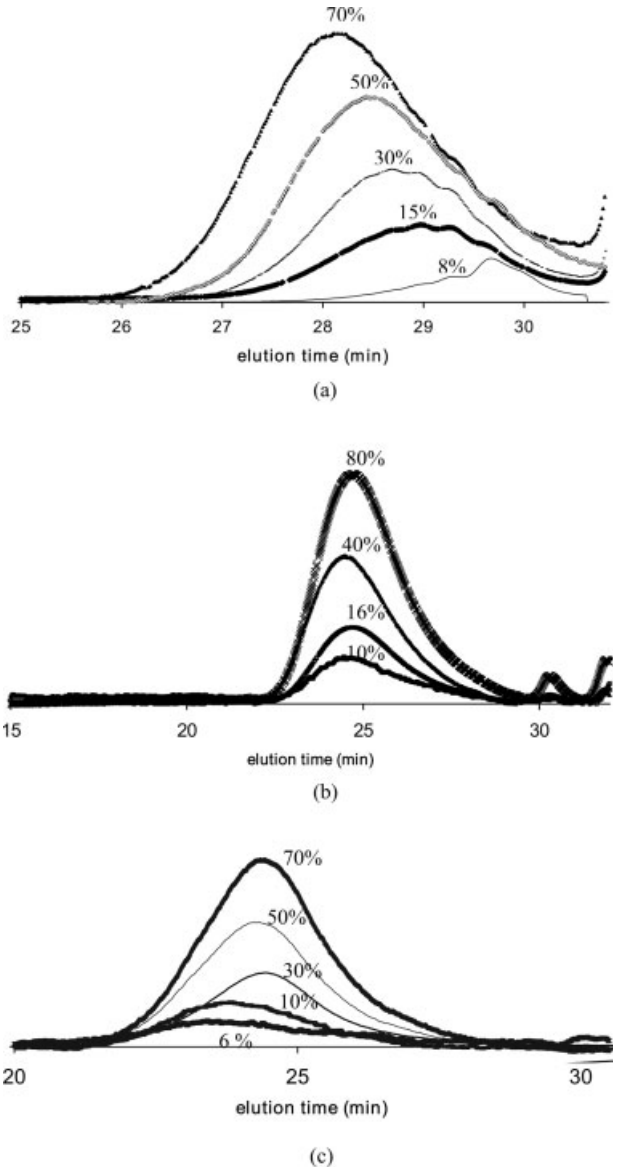

Figure 2. SEC chromatograms for various ITPs of VDF with different CTAs (the percentages are the α_{VDF} values): (a) PVDF–I obtained from the polymerization of VDF with $C_6F_{13}I$ initiated with TBPPI at 75 °C (experimental condition for the ITP of VDF: $[VDF]_0/[C_6F_{13}I]_0/[TBPPI]_0 = 100.00:6.60:0.66$), (b) PVDF–I obtained from the polymerization of VDF with $HCF_2CF_2CH_2I$ initiated with TBPPI at 75 °C (experimental condition for the ITP of VDF: $[VDF]_0/[HCF_2CF_2CH_2I]_0/[TBPPI]_0 = 100.00:6.60:0.66$), and (c) PVDF–I obtained from the polymerization of VDF with $HCF_2CF_2CH_2I$ initiated with DHPB at 135 °C (experimental condition for the ITP of VDF: $[VDF]_0/[HCF_2CF_2CH_2I]_0/[DHPB]_0 = 100.00:6.60:0.66$).

the monoadduct arose from the same coupling constants ($^3J_{HF} = {}^4J_{FF} = 10.0$ Hz), in contrast to the triplets ($^3J_{HF} = 15.0$ Hz) of triplets ($^4J_{FF} = 13.0$ Hz)[47,52] of the same signal in the diadduct and the triadduct. This difference can be explained by the electronegativity effect of the CTA (i.e., $C_6F_{13}I$) on the end group ($—CF_2I$). Figure 4(b) also presents the ^{19}F NMR spectrum in these PVDF–I polymers after the irradiation of the fluorine atoms in the $—CF_2I$ group, and the series of triplets ($^3J_{HF} = 15.0$ Hz) confirms these assignments.

Thus, it was possible to monitor the CTA consumption versus time by the shift of the peak corresponding to signals of $—CH_2—CF_2I$ end groups centered at −40 ppm ($C_6F_{13}CH_2CF_2I$) to −38 ppm [$C_6F_{13}(CH_2CF_2)_nI$]. The CTA was quickly consumed.

As discussed previously, the experimental $DP_{n,^{19}F}$ NMR values linearly increased with α_{VDF} [Fig. 1(a)] and were close to the theoretical ones. Actually, the evolutions of DP_n versus α_{VDF} in the ITPs of VDF achieved in the presence of both $C_6F_{13}I$ and $C_6F_{13}CH_2CF_2I$ are similar [Fig. 1(a)]. This shows that the reactivities of these two CTAs are close. Hence, in the course of transfer reactions, chains terminated by a $—CH_2CF_2I$ end group are involved in a controlled radical polymerization.

As in the case of $C_6F_{13}I$, the SEC chromatograms gave a shift of the oligomeric distribution toward the lower elution times (i.e., toward an increase in DP_n or in the molar mass) versus the monomer conversions, in agreement with the results of ^{19}F NMR. This statement confirms the controlled character of the ITP reaction performed in the presence of $C_6F_{13}CH_2CF_2I$. The PDI values were close to 1.2 even after 50 min ($\alpha_{VDF} \approx 95\%$, $\alpha_{CTA} = 1$) at 75 °C.

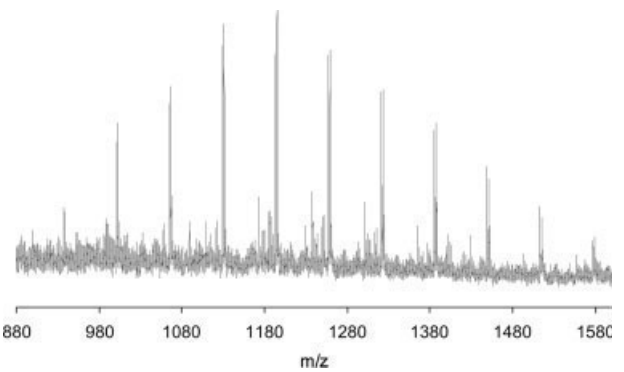

Figure 3. MALDI-TOF mass spectrum of low-molecular-weight C_6F_{13}–$(VDF)_n$–I ($DP_{n,^{19}F}$ NMR = 12; experimental condition for the ITP of VDF: $[VDF]_0/[C_6F_{13}I]_0/[TBPPI]_0 = 100.00:6.60:0.66$). The analysis was performed in the reflectron mode.

10990518, 2006, 19, Downloaded from https://onlinelibrary.wiley.com/doi/10.1002/pola.21654 by Cochrane Japan, Wiley Online Library on [30/05/2023]. See the Terms and Conditions (https://onlinelibrary.wiley.com/terms-and-conditions) on Wiley Online Library for rules of use; OA articles are governed by the applicable Creative Commons License

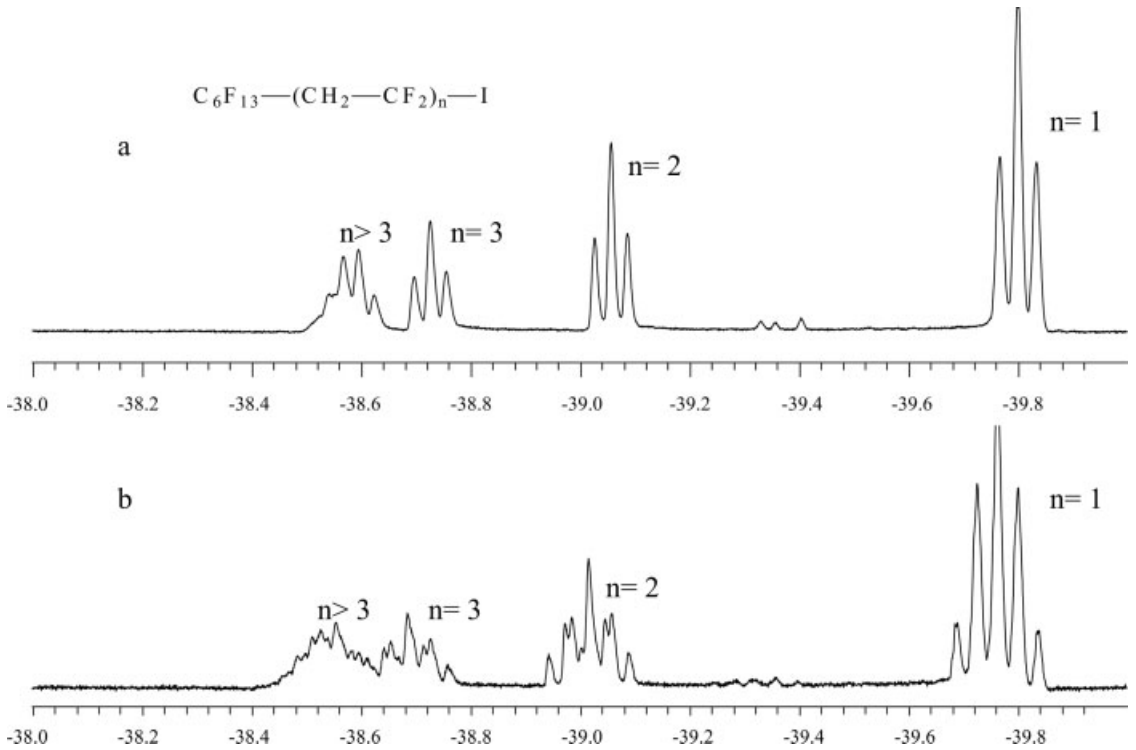

Figure 4. Expansion of the −38 to −40 ppm zone in the ^{19}F NMR spectra of the oligomer obtained by the ITP of VDF with the CTA $C_6F_{13}CH_2CF_2I$ at 75 °C (400 MHz, 298 K, in deuterated DMSO): (a) after the irradiation of the proton in $-CH_2CF_2I$ and (b) without any irradiation of the proton.

Furthermore, MALDI-TOF analysis was performed on a sample obtained by the ITP of VDF with this CTA. The result was similar to that involving $C_6F_{13}I$ as the CTA. We have noted the absence of the peaks assigned to oligomers obtained by direct initiation.

ITP of VDF in the Presence of $HCF_2CF_2CH_2I$

Two ITPs of VDF were achieved at 75 and 135 °C, initiated with TBPPI and DHBP, respectively. The temperatures of these ITPs were chosen because these radical initiators exhibit half-lives of 1 h. The conversion of $HCF_2CF_2CH_2I$ was monitored by ^{19}F NMR, and we took into account the integral of the signal centered at −136.0 ppm and attributed to the HCF_2- α group of the polymer, which underwent a slight high-field shift to −138.0 ppm of the CTA (see Fig. 7 in the supplementary material).

In contrast to both cases previously described, the $HCF_2CF_2CH_2I$ consumption versus α_{VDF} (Fig. 6 in the supplementary material) was much slower and may have evidenced a lower value of C_{Tr} than those of both CTAs bearing an ω-CF_2I group. However, an increase in the temperature slightly increased α_{CTA}. This statement was confirmed by the plotting of the evolution of DP_n, ^{19}F NMR values versus α_{VDF} at 75 and 135 °C. The experimental DP_n values of both these experiments were far from the theoretical ones and could indicate that C_{Tr} of $HCF_2CF_2CH_2I$ was lower than 1 [Fig. 1(b)]. Moreover, at high monomer conversions, the experimental DP_n values obtained at 75 and 135 °C were close.

Figure 2(b,c) presents the SEC chromatograms of oligomers produced from the ITPs of VDF carried out in the presence of $HCF_2CF_2CH_2I$ at 75 and 135 °C, respectively. The oligomeric distributions did not shift toward higher molar masses versus the monomer conversion, in contrast to reactions carried out in the presence of the other CTAs ($C_6F_{13}I$ and $C_6F_{13}CH_2CF_2I$). This result confirmed the poor control of ITP with $HCF_2CF_2CH_2I$ and could be correlated to Litvinenko and Mueller's theory.[49] Indeed, the PDI values were close to 2.0 (with polystyrene calibration) and confirmed the poor control of this radical polymerization with this CTA.

10990518, 2006, 19, Downloaded from https://onlinelibrary.wiley.com/doi/10.1002/pola.21654 by Cochrane Japan, Wiley Online Library on [30/05/2023]. See the Terms and Conditions (https://onlinelibrary.wiley.com/terms-and-conditions) on Wiley Online Library for rules of use; OA articles are governed by the applicable Creative Commons License

This result was confirmed by MALDI-TOF. In contrast to the previous spectra, a Gaussian distribution was not observed (Fig. 5), and the spectrum of $HCF_2CF_2CH_2$–$(VDF)_n$–I oligomers (Fig. 5) shows a series of peaks separated by 64 Da, which corresponds to the molecular weight of the VDF monomer unit. The expansion of the zone ranging from 1200 to 1264 Da exhibits three different series (A–C) that can be distinguished (Fig. 5).

The expected $HCF_2CF_2CH_2$–$(VDF)_{15}$–I/Na^+ structure (series B, Fig. 5) appears at 1225.28. This structure was confirmed by ^{19}F NMR analysis. Similar structures stem from the following equation: 1225.28 + $m \times 64$ Da (with m ranging from 1 to 7). Indeed, in the ITP reaction, the polymerization of VDF can be initiated by the radicals obtained from the decomposition of TBPPI [$CH_3^\bullet$ or $^\bullet C(CH_3)_3$].[51] The distribution at 1205.27 + $y \times 64$ Da (with y ranging from 0 to 7; series A, Fig. 5) could be ascribed to the coupling of CH_3–$(VDF)_n^\bullet$ with another CH_3–$(VDF)_m^\bullet$ radical to give CH_3–$(VDF)_{n+m}$–CH_3/Na^+, with $n + m = 18$. This hypothesis was confirmed by ^1H NMR spectra (see Figs. 7 and 8 in the supplementary material), in which the characteristic signals centered at 1.0, 1.2, 1.3, and 1.8 ppm were assigned to $(CH_3)_3C—CH_2$, $(CH_3)_3C—CF_2—$, $CH_3—CH_2—$, and $CH_3—CF_2—$ groups, respectively.[51] The $(CH_3)_3C$–$(VDF)_{n+m}$–$C(CH_3)_3/Na^+$ structures gave signals at 1225.28 and 1289.29 Da. These distributions overlapped that of the $HCF_2CF_2CH_2$–$(VDF)_n$–I/Na^+. The distribution at 1245.28 Da (series C, Fig. 5) could be attributed to the $(CH_3)_3C$–$(VDF)_{n+m}$–CH_3/Na^+structure, which was generated by the coupling of CH_3–$(VDF)_n^\bullet$ with CH_3–$(VDF)_m^\bullet$ radicals. Hence, there is a competition between the transfer reaction and the direct initiation. Thus, MALDI-TOF spectroscopy confirmed the poor efficiency of $HCF_2CF_2CH_2$–I as the CTA in the ITP of VDF.

Assessment of the C_{Tr} Values of Iodofluorinated CTAs and C_{ex} Values of PVDF–I

The literature reports several methods for assessing C_{Tr} values, such as those developed by Mayo,[53] O'Brien and Gornick,[54] David and Gosselain,[55] Bauduin et al.,[56] and Maeder and Gilbert,[57] but none of them took the living character into account because they were applied only for telomerization.[58] For controlled radical polymerizations such as ITP or RAFT, this becomes more complex

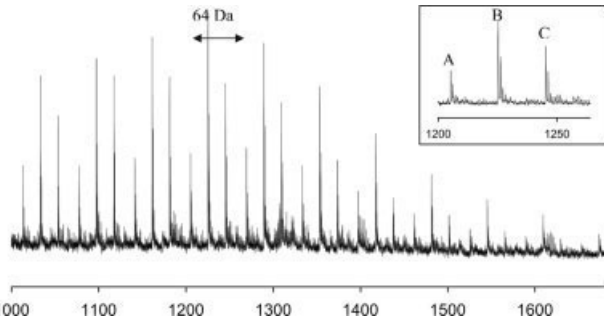

Figure 5. MALDI-TOF mass spectrum of $HCF_2CF_2CH_2$–$(VDF)_n$–I ($DP_n = 32$, as assessed by ^{19}F NMR; experimental condition for the ITP of VDF at 75 °C: $[VDF]_0/[HCF_2CF_2CH_2I]_0/[TBPPI]_0 = 100.00:6.60:0.66$; targeted $DP_n = 15$). The analysis was performed in the reflectron mode. The A series corresponds to the CH_3–$(VDF)_{n+m}$–CH_3/Na^+ structure. The B series corresponds to the $HCF_2CF_2CH_2$–$(VDF)_{15}$–I/Na^+ and $(CH_3)_3C$–$(VDF)_{n+m}$–$C(CH_3)_3/Na^+$ structures. The C series corresponds to the $(CH_3)_3C$–$(VDF)_{n+m}$–CH_3/Na^+structure.

because the dormant chains also act as transfer agents (Scheme 3). In the ITP mechanism, two different transfer reactions can occur, and we must well differentiate these two reactions:

1. The first one is based on the CTA itself and is defined by C_{Tr} ($C_{Tr} = k_{tr}/k_p$). C_{Tr} is actually ascribed to the activity of the iodinated transfer agent, and thus it determines the evolution of DP_n versus the monomer conversion (see Fig. 10 in the supplementary material). There are two cases: if C_{Tr} is very low ($C_{Tr} < 1$), the CTA consumption is slow, and the experimental molar masses will start high (and with very different values from the targeted ones) and decrease versus the monomer conversion. On the contrary, if C_{Tr} is high ($C_{Tr} > 1$), the experimental molar masses will increase almost linearly versus the monomer conversion and will be close to the targeted values.
2. The second one occurs between two polymeric chains (degenerative transfer) and is defined by C_{ex} ($C_{ex} = k_{ex}/k_p$). Unlike C_{Tr}, C_{ex} is characteristic of the degenerative transfer, that is, the evolution of the molecular weight distribution versus the monomer conversion. It is noteworthy that an increase in C_{ex} gives a lower PDI of the polymeric chains (see Fig. 11 in the supplementary material).

10990518, 2006, 19, Downloaded from https://onlinelibrary.wiley.com/doi/10.1002/pola.21654 by Cochrane Japan, Wiley Online Library on [30/05/2023]. See the Terms and Conditions (https://onlinelibrary.wiley.com/terms-and-conditions) on Wiley Online Library for rules of use; OA articles are governed by the applicable Creative Commons License

Determination of C_{Tr}

In this work, O'Brien and Gornick's method[54] was used to determine the C_{Tr} constant. This method was previously used by Chong et al.[12] to determine the high C_{Tr} value of a dithiobenzoate used in the RAFT polymerization of styrene and methyl methacrylate (MMA). Actually, this kind of controlled radical polymerization requires a transfer step as in the case of ITP. These authors monitored both the CTA and monomer consumptions, and plotting ln [CTA] versus ln [VDF] led to a straight line, the slope of which gave C_{Tr} (eqs 5 and 6, the demonstration being given in the supplementary material):

$$\frac{R_p/[VDF]}{R_{tr}/[CTA]} = \frac{k_p}{k_{tr}} = \frac{1}{C_{Tr}} \quad (5)$$

where [VDF] and [CTA] represent the monomer and transfer agent concentrations, respectively, and R_p and R_{tr} stand for the propagation and transfer rates, respectively.

After integration, eq 5 gives

$$\ln([CTA]_0/[CTA]) = C_{Tr} \ln([VDF]_0/[VDF]) \quad (6)$$

This method was successfully used for this investigation, and monitoring the ITP of VDF with three CTAs (Fig. 6) led to different values of C_{Tr} (Table 1). The C_{Tr} values of $C_6F_{13}I$ and of $C_6F_{13}CH_2CF_2I$ were rather close (7.9 and 7.4 at 75 °C, respectively), whereas that of $HCF_2CF_2CH_2I$ was much lower (0.3 and 0.4 at 75 and 135 °C, respectively, Table 1). Thus, the C_{Tr} value of a CTA bearing a $-CF_2I$ end group ($C_{Tr} \sim 7.7$ at 75 °C) was about 20 times higher than that of a CTA terminated by $-CF_2CH_2I$ ($C_{Tr} \sim 0.3$ and 0.4 at 75 and 135 °C, respectively).

An alternative method for assessing C_{Tr} is based on the evolution of DP_n versus the monomer conversion (eq 7), as suggested by Mueller and coworkers.[49,59,60] This method arises from the Bauduin et al.'s law[56] established in the 1980s for the telomerization process. Litvinenko and Mueller[49] demonstrated that eq 7 can be used to assess the C_{Tr} value in the case of degenerative transfer polymerizations, whatever the polymerizations (i.e., anionic, cationic, group transfer, and radical polymerization):

$$DP_n \approx \frac{\frac{[VDF]_0}{[CTA]_0} \times \alpha_{VDF}}{1 - \left(1 - \frac{([P^\circ])}{[CTA]_0}\right) \times (1 - \alpha_{VDF})^{C_{Tr}}} \quad (7)$$

where $[P^\circ]$ represents the concentration of macroradicals at a given time.

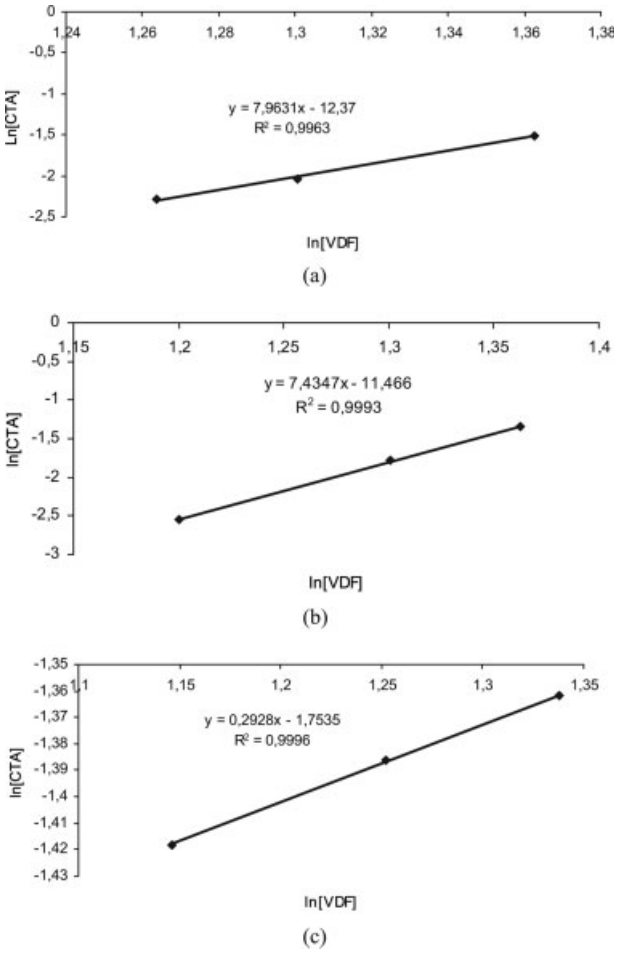

Figure 6. Plots of ln [CTA] versus ln [VDF] for the ITP of VDF at 75 °C initiated with TBPPI in the presence of three different CTAs: (a) $C_6F_{13}I$, (b) $C_6F_{13}CH_2CF_2I$, and (c) $HCF_2CF_2CH_2I$ (experimental condition for the ITP of VDF: $[VDF]_0/[CTA]_0/[TBPPI]_0 = 100.00:6.60:0.66$). The C_{Tr} values were evaluated with the method of O'Brien and Gornick.[54]

In the case of radical polymerization, eq 7 can be simplified to obtain Bauduin's equation (eq 8, the demonstration being given in the supplementary material). Indeed, in radical polymerization, the concentration of the radicals, $[P^\circ]$, is negligible (typically $< 10^{-6}$ mol L^{-1}), and thus the value of $1 - ([P^\circ]/[CTA]_0)$ is close to 1:

$$DP_n \approx \frac{\frac{[VDF]_0}{[CTA]_0} \cdot \alpha_{VDF}}{1 - (1 - \alpha_{VDF})^{C_{Tr}}} \quad (8)$$

The C_{Tr} values of the CTAs were obtained by the fitting of the experimental curves with eq 8. A comparison of the theoretical and experimental curves is given in the supplementary material. A good agreement was obtained between

10990518, 2006, 19, Downloaded from https://onlinelibrary.wiley.com/doi/10.1002/pola.21654 by Cochrane Japan, Wiley Online Library on [30/05/2023]. See the Terms and Conditions (https://onlinelibrary.wiley.com/terms-and-conditions) on Wiley Online Library for rules of use; OA articles are governed by the applicable Creative Commons License

Table 1. Assessments of the C_{Tr} Values of CTAs for the ITP of VDF[a]

CTA	Temperature (°C)	C_{Tr}	C_{ex}
$C_6F_{13}I$	75	7.9[b] (7.5[c])	—
$C_6F_{13}CH_2CF_2I$	75	7.4[b,c]	7.4 (PVDF–CH_2CF_2I)
$HCF_2CF_2CH_2I$	75	0.3[b,c]	0.3 (PVDF–CF_2CH_2I)
$HCF_2CF_2CH_2I$	135	0.4[b,c]	—

[a] Experimental condition: $[VDF]_0/[CTA]_0/[TBPPI]_0 = 100.00:6.60:0.66$.
[b] According to O'Brien and Gornick's method.[54]
[c] According to Litvinenko and Mueller's method.[49]

the C_{Tr} values determined by O'Brien and Gornick's method[54] and the Litvinenko and Mueller's method[49] (Table 1).

Determination of C_{ex} of PVDF–I

The C_{ex} value can be determined by the polymerization being started from a macrotransfer agent with the same structure as that of the dormant polymeric chains because, in this case, C_{Tr} is equal to C_{ex}. Fukuda and coworkers[48,61–63] used O'Brien and Gornick's method[54] to monitor the consumption of the macrotransfer agent, that is, polystyrene oligomers with an iodine end atom (PS–I), by SEC chromatography versus monomer conversion, and they assessed the C_{ex} value. For instance, this method was used to determine C_{ex} of PS–I ($C_{ex} = 3.4$ in the polymerization of styrene[48]). Boutevin and coworkers[64,65] used a poly(methyl acrylate)–I macrotransfer agent in the polymerization of methyl acrylate and applied Mayo's method to assess $C_{ex} = 2.2$ for poly(methyl acrylate)–I at 70 °C.[64] The same method was used to assess $C_{ex} = 2.6$ for poly(methyl methacrylate)–I at 80 °C.[65]

In this case, because $C_6F_{13}CH_2CF_2I$ mimics the PVDF–I dormant chains bearing a normal terminal VDF unit, the value of C_{Tr} for this CTA allows us to approximate C_{ex} of PVDF–CH_2CF_2–I (normal dormant species). Thus, C_{ex} for normal PVDF–I is approximately 7.4 at 75 °C.

Moreover, because $HCF_2CF_2CH_2I$ mimics the PVDF–I dormant chain bearing a reversed terminal VDF unit, the C_{Tr} value of this CTA allows us to assess C_{ex} of PVDF–CF_2CH_2I (reversed dormant chains): thus, C_{ex} for reversed PVDF–I is approximately 0.3 at 75 °C. To the best of our knowledge, this is the first time that C_{ex} values have been determined for the ITP of VDF.

This study also enables us to understand why oligomers of low DP_n values contain only a —CH_2I end group. Indeed, in the course of the ITP of VDF, two macromolecular transfer agents have been produced (bearing either —CF_2I or —CH_2I end groups), and they do not exhibit the same reactivity. Hence, when the reaction medium contains macromolecular chains terminated by —CF_2I, the polymerization almost exclusively occurs on these end groups rather than on the poorly reactive —CH_2I end groups.

Mechanism of ITP of VDF

Among the growing PVDF–I chains in the reaction medium, the presence of two types of end groups (—CF_2I and —CH_2I) can be observed. To confirm and check the different reactivities of these structures and also to investigate the competition between them, the ITP of VDF was carried out in the presence of stoichiometric amounts of $C_6F_{13}I$ and $HC_2F_4CH_2I$ as the CTAs. Methyl ethyl ketone was chosen as the solvent (which allowed us to preserve the solubility of high-molar-mass PVDF, thus leading to a homogeneous mixture), and it was initiated with TBPPI. As previously stated, both α_{CTA} and α_{VDF} were monitored by ^{19}F NMR. Figure 7 presents the conversion versus time for several species present in the reaction medium, allowing us to understand better the mechanism of the ITP of VDF when both CTAs and oligomers possess —CF_2I and —CH_2I end groups.

Figure 7 shows that the ITP of VDF occurs according to three steps:

1. At the beginning of the reaction, $C_6F_{13}I$ was quickly consumed, whereas the concentration of $HC_2F_4CH_2I$ remained constant. This behavior confirms the high reactivity of $C_6F_{13}I$ ($C_{Tr} = 7.9$ at 75 °C) compared with that of $HC_2F_4CH_2I$ ($C_{Tr} = 0.3$ at 75 °C).

10990518, 2006, 19, Downloaded from https://onlinelibrary.wiley.com/doi/10.1002/pola.21654 by Cochrane Japan, Wiley Online Library on [30/05/2023]. See the Terms and Conditions (https://onlinelibrary.wiley.com/terms-and-conditions) on Wiley Online Library for rules of use; OA articles are governed by the applicable Creative Commons License

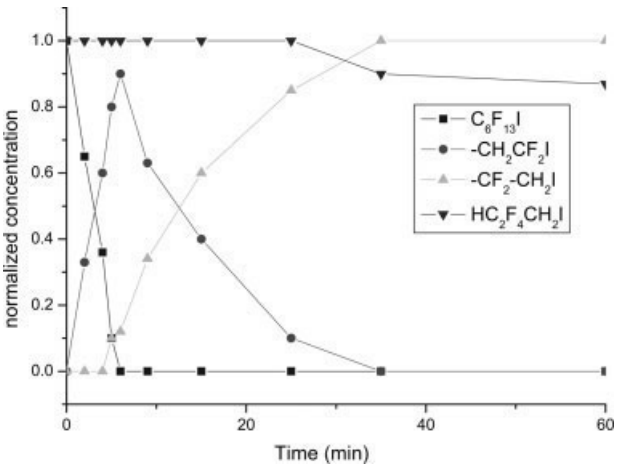

Figure 7. Evolution of the normalized concentrations of CTAs $C_6F_{13}I$ and $HC_2F_4CH_2I$ and oligomers bearing $—CH_2I$ and $—CF_2I$ end groups versus time for the ITP of VDF initiated with TBPPI at 75 °C. The normalized concentration represents the ratio of the concentrations at different times to the concentration at the initial time.

2. In a second stage, after the consumption of $C_6F_{13}I$, the transfer reaction took place on the oligomers bearing a $—CH_2CF_2I$ end group, whereas $HC_2F_4CH_2I$ still did not react significantly. Because of the lower reactivity of the reversed dormant chains (i.e., PVDF–CF_2CH_2I), the number of $—CH_2CF_2I$ end groups decreased versus time, whereas the concentration of PVDF–CF_2CH_2I increased. This second step lasted until the DP_n value was about 40, at which the concentration of the $—CH_2CF_2I$ end groups vanished, whereas that of the $—CF_2CH_2I$ end groups reached its maximum.
3. In a last stage, because of the low C_{Tr} value of $HCF_2CF_2CH_2I$, only a small number of new polymeric chains were created (small effect on DP_n). However, the low C_{ex} value of the PVDF–CF_2CH_2I dormant chains now led to a slow exchange between active and dormant chains, and therefore the molecular weight distribution became poorly controlled (increase in PDI) (Figure 12 of the supplementary material).

These results confirm the difference in the reactivities of the different CTAs. Thus, it is possible to classify the reactivities of the end groups in the following decreasing order: $—CF_2CF_2I > —CH_2CF_2I \gg —CF_2CH_2I$.

In conclusion, the ITP of VDF occurs according to two stages. In the first stage, when $—CF_2I$ end-group species are still present in the reaction medium, the polymerization is well controlled. This behavior corresponds to a conventional ITP mechanism. On the contrary, in the second stage, when $—CF_2I$ end-group species are almost totally consumed, the $—CH_2I$ end-group species can still transfer, but the exchange between active and dormant chains becomes slower than propagation ($C_{ex} < 1$). Thus, the polymerization is no longer controlled, and this second behavior is closer to that of a telomerization mechanism. However, in the second stage of the polymerization, because $—CF_2I$ end groups can be created again by a new inversion, the controlled character of the polymerization is preserved to some extent.

Assessment of $k_p/\sqrt{k_{te}}$ for the VDF for ITP

The evolution of $\ln([VDF]_0/[VDF])$ versus time (Fig. 8) is linear and shows that the macromolecular radical concentration, $[P^\circ]$, is constant. The slope of the straight line led to the assessment of $k_p \times [P^\circ] = 5 \times 10^{-4}\ s^{-1}$ at 75 °C (Fig. 8).

In radical polymerization, $k_p/\sqrt{k_{te}}$ usually represents the reactivity of the monomer. The overall rate of polymerization depends on the kinetic constant: $k = k_p/\sqrt{k_{te}}$. Such a value can be assessed with Tobolsky's equation:[66,67]

$$\ln\frac{[M]_0}{[M]} = 2\frac{k_p}{\sqrt{k_{te}}}\sqrt{\frac{f}{k_d}}\sqrt{[TBPPI]_0}[1-\exp(-k_d \cdot t/2)] \quad (9)$$

where f, k_d, and t represent the efficiency, the decomposition rate coefficient of the initiator,

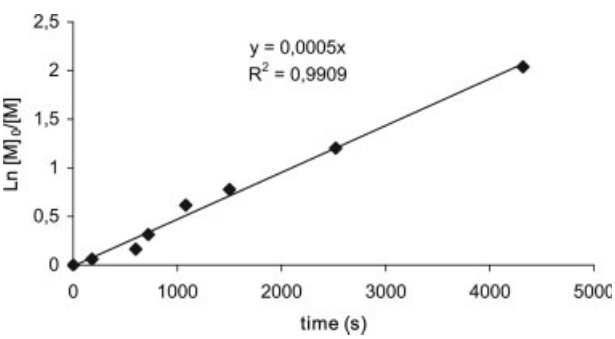

Figure 8. Plots of $\ln([M]_0/[M])$ versus time for the ITP of VDF initiated with TBPPI in the presence of $HCF_2CF_2CH_2I$ at 75 °C (for the assessment of the apparent propagation rate constant, $k_p^{app} = k_p[P^\circ] = 5.10^{-4}\ s^{-1}$; experimental condition for the ITP of VDF: $[VDF]_0/[HCF_2CF_2CH_2I]_0/[TBPPI]_0 = 100.00:6.60:0.66$).

10990518, 2006, 19, Downloaded from https://onlinelibrary.wiley.com/doi/10.1002/pola.21654 by Cochrane Japan, Wiley Online Library on [30/05/2023]. See the Terms and Conditions (https://onlinelibrary.wiley.com/terms-and-conditions) on Wiley Online Library for rules of use; OA articles are governed by the applicable Creative Commons License

and time, respectively (the other symbols being defined previously).

Thus, plotting $\ln([M]_0/[M])$ versus $1 - \exp[(-k_d t)/2]$ enabled us to assess the $k_p/\sqrt{k_{te}}$ value from the slope of the obtained straight line. Taking into account $f = 0.9$, $k_d = 2.79 \times 10^{-4}$ s^{-1},[68] and $[TBPPI]_0 = 2.6 \times 10^{-2}$ mol L^{-1}, we find a value of $k_p^2/k_{te} = 1.9 \times 10^{-2}$ L mol^{-1} s^{-1} at 75 °C. To the best of our knowledge, this is the first value for the radical polymerization of VDF supplied in the literature.

Taking into account k_p^2/k_{te} values, we can consider VDF a reactive monomer in comparison with other usual monomers, such as styrene ($k_p^2/k_{te} = 2.23 \times 10^{-3}$ L mol^{-1} s^{-1} at 70 °C)[69–71] or MMA ($k_p^2/k_{te} = 3.1 \times 10^{-2}$ L mol^{-1} s^{-1} at 80 °C).[72]

CONCLUSIONS

This work highlights the existence of two different mechanisms for the ITP of VDF. Hence, the kinetics of this reaction were determined in the presence of three different transfer agents. The reactivities of $C_6F_{13}I$ and $C_6F_{13}CH_2CF_2I$ were rather close, and these CTAs were quickly and totally consumed at 75 °C. In addition, the evolutions of DP_n versus the monomer conversion were similar and linear. Thus, the controlled character of the radical polymerization of VDF in the presence of these transfer agents was proved. However, reverse additions of the macroradical onto VDF were also observed. This reaction was evidenced by the presence of $—CH_2–I$ end groups in PVDF–I, leading to an unfavorable ITP process. Indeed, in the case of the ITP of VDF in the presence of the $HCF_2CF_2CH_2I$ transfer agent, the DP_n evolution versus α_{VDF} was similar to that of a telomerization. This statement was also confirmed by a low C_{Tr} value of $HCF_2CF_2CH_2I$ (<1), which allowed nevertheless the polymeric chains to preserve a controlled character in the course of the polymerization. Furthermore, with O'Brien and Gornick's method, the C_{Tr} values of these three CTAs were assessed. $C_6F_{13}I$ and $C_6F_{13}CH_2CF_2I$ had similar C_{Tr} values (ca. 7.7 at 75 °C) whereas that of $HCF_2CF_2CH_2I$ was much lower (0.3 or 0.4 at 75 or 135 °C, respectively). C_{ex} of PVDF–CH_2CF_2I dormant chains was estimated to be $C_{ex} \approx C_{Tr}$ ($C_6F_{13}CH_2CF_2I$) = 7.4 at 75 °C, whereas C_{ex} of PVDF–CF_2CH_2I dormant chains was approximated to be $C_{ex} \approx C_{Tr}$ ($HCF_2CF_2CH_2I$) = 0.3 at 75 °C. Having carried out the ITP of VDF in the presence of CTAs $C_6F_{13}I$ and $HCF_2CF_2CH_2I$, we can propose a general mechanism for the ITP of VDF in two stages. The first stage corresponds to a conventional ITP mechanism in which $C_6F_{13}I$ is first mainly consumed, and this is followed by the produced oligomers bearing $—CF_2I$ end groups. The second stage occurs once the concentration of $—CF_2I$ species becomes negligible, and the polymerization then mainly proceeds as a telomerization, in which species bearing $—CH_2I$ end groups behave as transfer agents. Finally, k_p^2/k_{te} of VDF was determined to be 1.9 $\times 10^{-2}$ L mol^{-1} s^{-1} at 75 °C. Further investigations of the synthesis of block copolymers from these PVDF–Is prepared by ITP are in progress.

The authors thank Solvay S.A. Co. (Brussels, Belgium, and Tavaux, France) for free samples of VDF and 1,1,1,3,3-pentafluorobutane, Akzo Nobel (Châlons sur Marne, France) for *tert*-butylperoxypivalate, Gilles Valette (University of Montpellier II) for matrix-assisted laser desorption/ionization time-of-flight analyses, and Alain Fruchier (the head of NMR for Ecole Nationale Supérieure de Chimie de Montpellier) for high-resolution NMR characterizations.

REFERENCES AND NOTES

1. Tatemoto, M.; Nakagawa, T. (Daikin Kogyo Co., Ltd.). German Offenlegungsschrift 2729671, 1978.
2. Tatemoto, M.; Suzuki, T.; Tomoda, M.; Furukawa, Y.; Ueta, Y. (Daikin Kogyo Co., Ltd.). German Offenlegungsschrift 2815187, 1978.
3. Tatemoto, M. Int Polym Sci Technol 1985, 12, 85–91.
4. Matyjaszewski, K. In Handbook of Radical Polymerization; Matyjaszewski, K.; Davis, T., Eds.; Wiley-Interscience: New York, 2002; p 361.
5. Hawker, C. J.; Bosman, A. W.; Harth, E. Chem Rev 2001, 101, 3661–3688.
6. Matyjaszewski, K.; Xia, J. Chem Rev 2001, 101, 2921–2990.
7. Kamigaito, M.; Ando, T.; Sawamoto, M. Chem Rev 2001, 101, 3689–3745.
8. Tatemoto, M.; Tomoda, M.; Ueta, Y. (Daikin Kogyo Co., Ltd.). German Offenlegungsschrift 2940135, 1980.
9. Tatemoto, M. Polymeric Materials Encyclopedia; Salamone, J. C., Ed.; CRC, Boca Raton, Florida, 1996, Vol 5, 3847–3860.
10. Charmot, D.; Corpart, P.; Adam, H.; Zard, S. Z.; Biadatti, T.; Bouhadir, G. Macromol Symp 2000, 150, 23–32.
11. Destarac, M.; Bzducha, W.; Taton, D.; Gauthier-Gillaizeau, I.; Zard, S. Z. Macromol Rapid Commun 2002, 23, 1049–1054.
12. Chong, Y. K.; Krstina, J.; Le, T. P. T.; Moad, G.; Postma, A.; Rizzardo, E.; Thang, S. H. Macromolecules 2003, 36, 2256–2272.

10990518, 2006, 19, Downloaded from https://onlinelibrary.wiley.com/doi/10.1002/pola.21654 by Cochrane Japan, Wiley Online Library on [30/05/2023]. See the Terms and Conditions (https://onlinelibrary.wiley.com/terms-and-conditions) on Wiley Online Library for rules of use; OA articles are governed by the applicable Creative Commons License

13. Chiefari, J.; Mayadunne, R. T. A.; Moad, C. L.; Moad, G.; Rizzardo, E.; Postma, A.; Skidmore, M. A.; Thang, S. H. Macromolecules 2003, 36, 2273–2283.
14. Ameduri, B.; Boutevin, B.Well-Architectured Fluoropolymers: Synthesis, Properties and Applications; Elsevier: Amsterdam, 2004.
15. Yagi, T.; Tsuda, N.; Noguchi, T.; Sakaguchi, K.; Tanaka, Y.; Tatemoto, M. (Daikin Industries, Ltd.). Eur. Pat. Appl. 422644, 1991.
16. Hung, M. H. (E. I. du Pont de Nemours and Co.). U.S. Patent 5,231,154, 1993.
17. Carlson, D. P. (E. I. du Pont de Nemours and Co.). U.S. Patent 5,284,920, 1994.
18. Arcella, V.; Brinati, G.; Albano, M.; Tortelli, V. (Ausimont SpA). Eur. Pat. Appl. 661312, 1995.
19. Arcella, V.; Brinati, G.; Albano, M.; Tortelli, V. (Ausimont SpA). Eur. Pat. Appl. 683186, 1995.
20. Gayer, U.; Schuh, T.; Arcella, V.; Albano, M. (Ausimont SpA). Eur. Pat. Appl. 885928, 1998.
21. Tatemoto, M. Int Polym Sci Technol 1985, 12, 85–91 (translated into English from Nippon Gomu Kyokaishi 1984, 57, 761–767).
22. Lansalot, M.; Farcet, C.; Charleux, B.; Vairon, J.-P.; Pirri, R. Macromolecules 1999, 32, 7354–7360.
23. Gaynor, S. G.; Wang, J.-S.; Matyjaszewski, K. Macromolecules 1995, 28, 8051–8056.
24. Farcet, C.; Lansalot, M.; Pirri, R.; Vairon, J. P.; Charleux, B. Macromol Rapid Commun 2000, 21, 921–926.
25. Percec, V.; Ramirez-Castillo, E.; Popov, A. V.; Hinojosa-Falcon, L. A.; Guliashvili, T. J Polym Sci Part A: Polym Chem 2005, 43, 2178–2184.
26. Coelho, J. F. J.; Silva, A. M. F. P.; Popov, A. V.; Percec, V.; Abreu, M. V.; Goncalves, P. M. O. F.; Gil, M. H. J Polym Sci Part A: Polym Chem 2006, 44, 2809–2825.
27. Iovu, M. C.; Matyjaszewski, K. Macromolecules 2003, 36, 9346–9354.
28. Lacroix-Desmazes, P.; Severac, R.; Boutevin, B. ACS Symp Ser 2003, 854, 570–585.
29. Bak, P. I.; Bidinger, G. P.; Cozens, R. J.; Klich, P. R.; Mayer, L. A. (Geon Co.). Eur. Pat. Appl. 617057, 1994.
30. Bak, P. I.; Bidinger, G. P.; Cozens, R. J.; Klich, P. R.; Mayer, L. A. (Geon Co.). U.S. Patent 5,455,319, 1995.
31. Percec, V.; Popov, A. V.; Ramirez-Castillo, E.; Weichold, O. J Polym Sci Part A: Polym Chem 2003, 41, 3283–3299.
32. Percec, V.; Popov, A. V. European Patent 1,406,935, 2004.
33. Percec, V.; Popov, A. V.; Ramirez-Castillo, E.; Coelho, J. F. J.; Hinojosa-Falcon, L. A. J Polym Sci Part A: Polym Chem 2004, 42, 6267–6282.
34. Percec, V.; Popov, A. V.; Ramirez-Castillo, E.; Weichold, O. J Polym Sci Part A: Polym Chem 2004, 42, 6364–6374.
35. Percec, V.; Guliashvili, T.; Popov, A. V. U.S. Patent 2,005,131,186, 2005.
36. Percec, V.; Popov, A. V.; Ramirez-Castillo, E. J Polym Sci Part A: Polym Chem 2005, 43, 287–295.
37. Percec, V.; Popov, A. V.; Ramirez-Castillo, E.; Coelho, J. F. J. J Polym Sci Part A: Polym Chem 2005, 43, 773–778.
38. Percec, V.; Popov, A. V.; Ramirez-Castillo, E.; Coelho, J. F. J.; Hinojosa-Falcon, L. A. J Polym Sci Part A: Polym Chem 2005, 43, 779–788.
39. Percec, V.; Guliashvili, T.; Popov, A. V.; Ramirez-Castillo, E. J Polym Sci Part A: Polym Chem 2005, 43, 1478–1486.
40. Percec, V.; Guliashvili, T.; Popov, A. V.; Ramirez-Castillo, E.; Coelho, J. F. J.; Hinojosa-Falcon, L. A. J Polym Sci Part A: Polym Chem 2005, 43, 1649–1659.
41. Percec, V.; Guliashvili, T.; Popov, A. V.; Ramirez-Castillo, E.; Hinojosa-Falcon, L. A. J Polym Sci Part A: Polym Chem 2005, 43, 1660–1669.
42. Percec, V.; Guliashvili, T.; Popov, A. V.; Ramirez-Castillo, E. J Polym Sci Part A: Polym Chem 2005, 43, 1935–1947.
43. Percec, V.; Guliashvili, T.; Popov, A. V. J Polym Sci Part A: Polym Chem 2005, 43, 1948–1954.
44. Percec, V.; Popov, A. V.; Ramirez-Castillo, E.; Hinojosa-Falcon, L. A. J Polym Sci Part A: Polym Chem 2005, 43, 2276–2280.
45. Coelho, J. F. J.; Silva, A. M. F. P.; Popov, A. V.; Percec, V.; Abreu, M. V.; Goncalves, P. M. O. F.; Gil, M. H. J Polym Sci Part A: Polym Chem 2006, 44, 3001–3008.
46. Boyer, C.; Valade, D.; Sauguet, L.; Ameduri, B.; Boutevin, B. Macromolecules 2005, 38, 10353–10362.
47. Balague, J.; Ameduri, B.; Boutevin, B.; Caporiccio, G. J Fluorine Chem 2000, 102, 253–268.
48. Goto, A.; Ohno, K.; Fukuda, T. Macromolecules 1998, 31, 2809–2814.
49. Litvinenko, G.; Mueller, A. H. E. Macromolecules 1997, 30, 1253–1266.
50. Monteiro, M. J. J Polym Sci Part A: Polym Chem 2005, 43, 5643–5651.
51. Guiot, J.; Ameduri, B.; Boutevin, B. Macromolecules 2002, 35, 8694–8707.
52. Ameduri, B.; Ladaviere, C.; Delolme, F.; Boutevin, B. Macromolecules 2004, 37, 7602–7609.
53. Mayo, F. R. J Am Chem Soc 1943, 65, 2324–2329.
54. O'Brien, J. L.; Gornick, F. J Am Chem Soc 1955, 77, 4757.
55. David, C.; Gosselain, P. A. Tetrahedron 1962, 18, 639–651.
56. Bauduin, G.; Boutevin, B.; Mistral, J. P.; Sarraf, L. Makromol Chem 1985, 186, 1445–1455.
57. Maeder, S.; Gilbert, R. G. Macromolecules 1998, 31, 4410–4418.
58. Boutevin, B.; Pietrasanta, Y.; Bauduin, G. Makromol Chem 1985, 186, 283–295.
59. Mueller, A. H. E.; Yan, D.; Litvinenko, G.; Zhuang, R.; Dong, H. Macromolecules 1995, 28, 7335–7338.

10990518, 2006, 19, Downloaded from https://onlinelibrary.wiley.com/doi/10.1002/pola.21654 by Cochrane Japan, Wiley Online Library on [30/05/2023]. See the Terms and Conditions (https://onlinelibrary.wiley.com/terms-and-conditions) on Wiley Online Library for rules of use; OA articles are governed by the applicable Creative Commons License

60. Mueller, A. H. E.; Zhuang, R.; Yan, D.; Litvinenko, G. Macromolecules 1995, 28, 4326–4333.
61. Fukuda, T.; Goto, A. ACS Symp Ser 2000, 768, 27–38.
62. Fukuda, T.; Goto, A.; Ohno, K. Macromol Rapid Commun 2000, 21, 151–165.
63. Fukuda, T.; Yoshikawa, C.; Kwak, Y.; Goto, A.; Tsujii, Y. ACS Symp Ser 2003, 854, 24–39.
64. Lacroix-Desmazes, P.; Severac, R.; Boutevin, B. Macromolecules 2005, 38, 6299–6309.
65. Boyer, C.; Lacroix-Desmazes, P.; Robin, J. J.; Boutevin, B. Macromolecules, 2006, 39, 4044–4053.
66. Tobolsky, A. V. J Am Chem Soc 1958, 80, 5927–5929.
67. Tobolsky, A. V.; Rogers, C. E.; Brickman, R. D. J Am Chem Soc 1960, 82, 1277–1280.
68. Bartlett, P. D.; Simons, D. M. J Am Chem Soc 1960, 82, 1753–1756.
69. Buback, M.; Gilbert, R. G.; Hutchinson, R. A.; Klumperman, B.; Kuchta, F.-D.; Manders, B. G.; O'Driscoll, K. F.; Russell, G. T.; Schweer, J. Macromol Chem Phys 1995, 196, 3267–3280.
70. Buback, M.; Kuchta, F.-D. Macromol Chem Phys 1995, 196, 1887–1898.
71. Buback, M.; Kuchta, F. D. Macromol Chem Phys 1997, 198, 1455–1480.
72. Buback, M.; Kowollik, C. Macromolecules 1998, 31, 3211–3215.

10990518, 2006, 19, Downloaded from https://onlinelibrary.wiley.com/doi/10.1002/pola.21654 by Cochrane Japan, Wiley Online Library on [30/05/2023]. See the Terms and Conditions (https://onlinelibrary.wiley.com/terms-and-conditions) on Wiley Online Library for rules of use; OA articles are governed by the applicable Creative Commons License